Chin. Phys. Lett. **39**, 047601 (2022)

Magnetic Phase Transition in Two-Dimensional $CrBr_3$ Probed by a Quantum Sensor

Haodong Wang(王浩东)[1,2†], Peihan Lei(雷沛涵)[1,2†], Xiaoyu Mao(毛晓宇)[1,3†], Xi Kong(孔熙)[4*], Xiangyu Ye(叶翔宇)[1,2], Pengfei Wang(王鹏飞)[1,2], Ya Wang(王亚)[1,2], Xi Qin(秦熙)[1,2], Jan Meijer[5], Hualing Zeng(曾华凌)[1,3*], Fazhan Shi(石发展)[1,2], and Jiangfeng Du(杜江峰)[1,2*]

[1]*Hefei National Laboratory for Physical Sciences at the Microscale and School of Physical Sciences, University of Science and Technology of China, Hefei 230026, China*
[2]*CAS Key Laboratory of Microscale Magnetic Resonance, University of Science and Technology of China, Hefei 230026, China*
[3]*CAS Center for Excellence in Quantum Information and Quantum Physics, University of Science and Technology of China, Hefei 230026, China*
[4]*National Laboratory of Solid State Microstructures and Department of Physics, Nanjing University, Nanjing 210093, China*
[5]*Felix-Bloch Institute for Solid State Physics, University Leipzig, Linné Str. 5, D-04103 Leipzig, Germany*

(Received 2 December 2021; accepted 14 February 2022; published online 28 March 2022)

Recently, magnetism in two-dimensional (2D) van der Waals (vdW) materials has attracted wide interests. It is anticipated that these materials will stimulate discovery of new physical phenomena and novel applications. The capability to quantitatively measure the magnetism of 2D magnetic vdW materials is essential to understand these materials. Here we report on quantitative measurements of ferromagnetic-to-paramagnetic phase transition of an atomically thin (down to 11 nm) vdW magnet, namely $CrBr_3$, with a Curie point of 37.5 K. This experiment demonstrates that surface magnetism can be quantitatively investigated, which is useful for a wide variety of potential applications.

DOI: 10.1088/0256-307X/39/4/047601

Magnetism of two-dimensional (2D) materials is an emergent phenomenon, which can be beneficial to numerous fields, including spintronics, quantum materials, heterostructures, and ultracompact storage.[1–6] Although the Mermin–Wagner theorem was believed to exclude the existence of 2D magnetism, anisotropic local 2D magnetism was observed in both CrI_3 and $Cr_2Ge_2Te_6$ in 2017.[7,8] However, a quantitative study of 2D magnetism under different external conditions is still required.[9,10] Phase transitions are observed under the application of both electrical gating[11–13] and a high stress,[14,15] whereas the stacking order may change the original magnetism.[16] Conventional methods used for probing bulk materials, such as superconducting quantum interference device magnetometry and neutron scattering, cannot easily measure the magnetism of tiny exfoliated atomic-layered films. Electrical transport measurements and magneto-optical Kerr effect imaging[17] both lack the ability to characterize the magnetization directly and quantitatively. Although the emergent spin-polarized scanning tunneling microscopy (STM) technique can measure magnetism directly on the atomic scale,[18] STM imaging can only be performed under ultrahigh vacuum conditions.

The 2D vdW magnet $CrBr_3$ is more stable than CrI_3[17] and is believed to be an ideal platform for investigating 2D magnetic materials. The Cr^{3+} ions form a hexagonal honeycomb lattice, and each ion is surrounded by six Br^- ions located at the corners of an octahedron, as shown in the inset of Fig. 1. The angle of the Br–Cr–Br bonds is 95.1°, indicating that the superexchange interaction between the Cr^{3+} ions is ferromagnetic.[19] The magnetic phase transition temperature T_C of bulk $CrBr_3$ has been reported to be 37 K. The long-range magnetic order is suppressed by the thermal magnons above T_C. In our experiment, thin layers of $CrBr_3$ were obtained via mechanical exfoliation. The Raman spectrum of these layers is shown in Fig. 1. The Raman peaks at 103 and 179 cm^{-1} correspond to the optical photon scattering from the A_g Raman modes, whereas the Raman peaks at 138 and 147 cm^{-1} are attributed to the scattering from the E_g Raman modes. The distinct sharp peaks are in excellent agreement with those observed in a typical Raman spectrum of the $CrBr_3$ crystal.

†These authors contributed equally to this work.
*Corresponding authors. Email: kongxi@nju.edu.cn; hlzeng@ustc.edu.cn; djf@ustc.edu.cn
© 2022 Chinese Physical Society and IOP Publishing Ltd

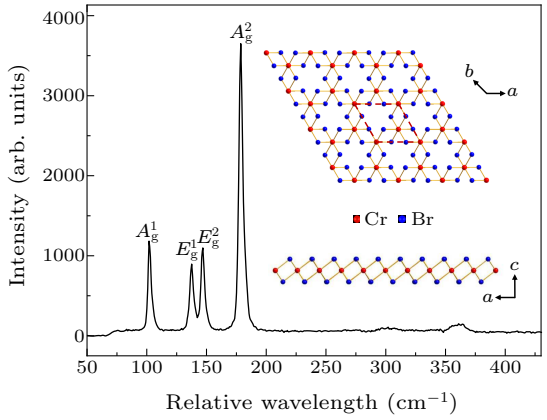

Fig. 1. Raman spectrum of $CrBr_3$. The peaks correspond to the A_g^1, E_g^1, E_g^2, and A_g^2 modes. The lattice structure of the $CrBr_3$ crystal is shown in the inset (top and side views). The red spheres represent the Cr^{3+} ions, whereas the blue spheres represent the Br^- ions.

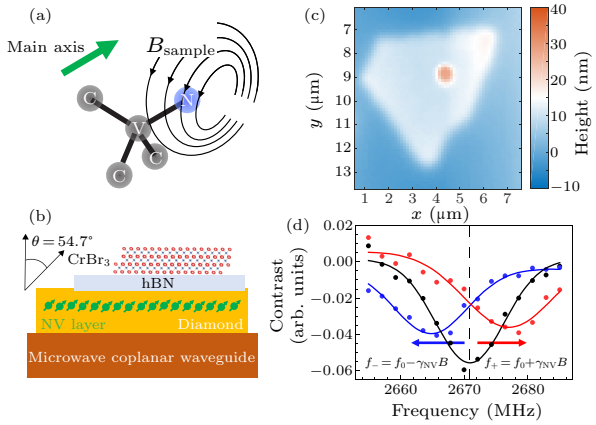

Fig. 2. Quantitative imaging of magnetism in the 2D vdW material $CrBr_3$. (a) A single NV electron spin is used as a magnetic sensor to probe magnetism. The observed frequency shift is $\Delta f = \gamma_e B_{NV}$, where B_{NV} is the component of the sample magnetic field B_{sample} projected onto the NV main axis. (b) A few layers of $CrBr_3$ are deposited on 160-nm-thick hBN layers. The whole sample is placed on a quantum magnetic sensor, which consists of a bulk diamond with a flat surface (within 5 nm). A layer of NV electron spins is implanted in diamond at a distance of 5–7 nm from the surface. (c) AFM image of $CrBr_3$ after the experiment. (d) ODMR spectra of the NV center. The black curve represents the spectrum in a region far away from the sample center at the resonant frequency $f_0 = D \pm \gamma_e B_{bias}$, where $D = 2870$ MHz is the zero-field splitting along the main axis of the NV electron spin. A positive or negative sample field B_{sample} shifts the spectrum, i.e., $f_\pm = f_0 \pm \gamma_e B_{sample}$.

Nitrogen-vacancy (NV) centers, which are atomic scale and highly magnetically sensitive quantum spin systems, have recently witnessed a considerable development in the fields of scanning magnetic imaging and magnetometry on the nanoscale.[20–24] NV centers provide a unique opportunity to measure the magnetization in a 2D plane.[25–29] The single-electron spin of the diamond NV center can be utilized to directly image the 2D magnetization distribution.[30] Furthermore, the magnetic domains and their evolution under an external magnetic field can be observed.[31] In this work, the diamond NV center was used to quantitatively measure the magnetism of a few-layer 2D material. In particular, the magnetization of few-layer $CrBr_3$ at different temperatures as well as the magnetic phase transition was directly observed.

The magnetic field generated by the vdW magnets was observed through the Zeeman splitting of the NV sensor. The NV center has a magnetically sensitive ground state. The Hamiltonian reads $H = DS_z^2 + \boldsymbol{B} \cdot \boldsymbol{S}$, where $D = 2870$ MHz is the zero-field splitting, $\boldsymbol{B}$ is the magnetic field, $\boldsymbol{S}$ is the vector electron spin operator, and $\boldsymbol{S} = (S_x, S_y, S_z)$. Furthermore, S_x, S_y, and S_z are the spin components of the NV electron spin. The experiment was performed under a static magnetic field B_{bias} along the main axis $\boldsymbol{e}_{NV}$. The magnetic field of the sample B_{sample} can be measured by determining the energy shift $f_\pm = D \pm \gamma_e B_{bias} \pm \gamma_e B_{sample}$ corresponding to the transition frequency between $m_s = 0$ and $m_s = \pm 1$, where the energy shift of the orthogonal field is suppressed by the large main axis energy splitting D. Thus, the component of the stray magnetic field $B_{sample} = B_{sample} \cdot \boldsymbol{e}_{NV}$ of the vdW magnet $CrBr_3$ projected along the NV main axis $\boldsymbol{e}_{NV}$ could be measured directly and quantitatively.

The sensing device in this experiment consisted of a thin diamond plate which was implanted with 5-keV nitrogen ions with a density of 3×10^{11} cm^{-2}. The diamond slab was [100]-oriented. After annealing at 800 ℃, a layer of the NV center ensemble was created within 5–7 nm from the diamond surface [Fig. 2(b)]. The sample consisted of an ultrathin layer of the vdW magnet $CrBr_3$ (with a minimum thickness of 11 nm) deposited on a thin layer of hexagonal boron nitride (hBN) [see the atomic force microscopy (AFM) image shown in Fig. 2(c) without hBN]. The bottom hBN layer was precisely measured to be 160 nm in thickness. The fabricated films were transferred onto the thin diamond plate above the NV center layer [Fig. 2(b)]. The whole system was placed in a liquid Helium-4 cryostat under an external magnetic bias field B_{bias} of 200 mT. The field direction was almost parallel to one of the main axes of the NV centers (i.e., the [111] axis). The measurement temperature was controlled to be in the range of 4–40 K using a feedback thermometer placed close to the sample. The optically detected magnetic resonance (ODMR) technique was used to detect the stray magnetic field B_{sample} of the vdW magnet $CrBr_3$. Firstly, using a confocal system, a 532-nm laser with a power of around 100 μW was focused on the NV center to excite and polarize it to the $m_s = 0$ spin

state. Secondly, the NV center was subjected to a microwave pulse with frequency f. When the microwave frequency f is resonant with the NV spin splitting $f_\pm = D \pm \gamma_e B_{\rm bias} \pm \gamma_e B_{\rm sample}$, the NV electron spin is excited to the $m_s = -1$ or $m_s = 1$ state (where a positive sign in the above expression corresponds to a negative sign in m_s, and vice versa), which exhibits a weak fluorescence. Finally, the fluorescence was collected using a confocal system, and the resonant frequency was observed. Thus, the magnetic field of the sample $B_{\rm sample} = \mp(f_\pm - D \mp \gamma_e B_{\rm bias})/\gamma_e$ could be determined by the ODMR, and the corresponding spectra are shown in Fig. 2(d).

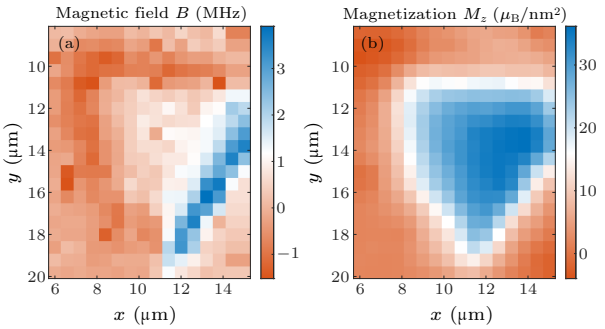

Fig. 3. Magnetization intensity maps of a thin layer of $CrBr_3$. (a) Sample magnetic field along the main axis $B_{\rm NV}$. The region shown corresponds to that illustrated in Fig. 2(c). (b) Surface magnetization density distribution $\sigma_s(x, y)$ reconstructed from the magnetic field map $B_{\rm NV}$.

Figure 3(a) shows the magnetic field map of a region containing $CrBr_3$ with a minimum thickness of 11 nm [indicated by the orange box in Fig. 2(c)]. The experiment was performed in a bias field $B_{\rm bias}$ of 200 mT at 4 K. The map was obtained by conducting NV ODMR measurements at each pixel (at a rate of around 3 min/pixel). The magnetic field was determined by $B_{\rm NV}(x, y, z = z_0)$, where z_0 is the distance between the NV layer and the 2D $CrBr_3$ layer. The magnetic field map shows that the stray magnetic fields emerge predominantly from the edges of the thin 2D $CrBr_3$ layer. We assume that the magnetization has only a perpendicular component under $B_{\rm bias} = 200$ mT. Thus, the magnetization distribution can be reconstructed from the stray field map $B_{\rm NV}$. A reverse propagation method was used to reconstruct the surface magnetization density distribution $\sigma_s(x, y)$ of the sample. The whole surface magnetization density distribution and the $\sigma_s(x, y)$ distribution of the $CrBr_3$ layer are shown in Fig. 3.

The thin $CrBr_3$ vdW sample was then measured at different temperatures, from 4 K to 40 K, to obtain the temperature response of the magnetization. We measured the magnetic stray field distributions at different temperatures, from which the corresponding surface magnetization density distributions of the thin material were reconstructed. The reconstructed surface magnetization density distributions at 4–35 K are shown in Figs. 4(a)–4(j). The surface magnetization density inside the material decreases as the temperature rises, and the magnetization almost vanishes at 35 K. This result indicates that the ferromagnetic-to-paramagnetic phase transition occurs at this temperature.

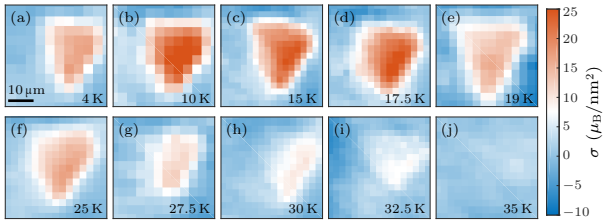

Fig. 4. Magnetism at different temperatures. (a)–(j) Surface magnetization density distribution $\sigma_s(x, y)$ of the region shown in Fig. 2(c) at different temperatures in the range of 4–35 K. The magnetism vanishes at 35 K.

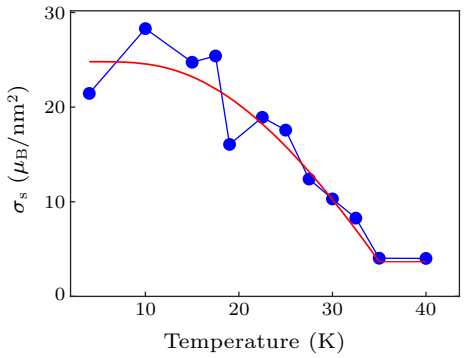

Fig. 5. Magnetic phase transition of the 2D vdW material. Magnetization density σ_s inside the 2D vdW material. The blue and red curves represent the experimental data and the fitting curve, respectively.

The average magnetization density σ_s at different temperatures is plotted in Fig. 5, and the magnetization almost vanishes at 35 K [Fig. 4(j)]. The anisotropic superexchange across the $\sim 90°$ Cr–Br–Cr bonds and the anisotropy of the Cr atoms with $S = 3/2$ open a gap Δ_0 in the spin wave spectrum, thus contributing to the emergent stable magnetism in 2D $CrBr_3$. The XXZ Heisenberg exchange model Hamiltonian adopted from Refs. [17,32] is $H = -(\sum D(S_i^z)^2 + J/2\sum_{i,j} \boldsymbol{S}_i \cdot \boldsymbol{S}_j + \lambda/2\sum_{i,j} S_i^z \cdot S_j^z)$, where D is the single-ion anisotropy, J is the exchange coupling, and λ is the anisotropic exchange. The Cr–Br–Cr bond angle and the positive exchange coupling ($J > 0$) indicate the existence of a ferromagnetic phase at low temperature, which is consistent with the magnetization distribution shown in Figs. 4(a)–4(j). The 2D $CrBr_3$ magnetization (μ_B per Cr atom) can be described as $M(T) = S - k_B T e^{-\Delta_0/k_B T}/2\pi JS$,[17,32] where $S = 3/2$, and k_B is the Boltzmann constant. Through fitting, the transition temperature of the $CrBr_3$ vdW material was found to be 37.5 K (Fig. 5), which is in agreement with the previous work.[33]

In summary, we have used an ensemble of NV centers to quantitatively investigate 2D magnetic materials. Nondestructive measurements on the nanoscale can be realized using our setup. Through these experiments, we observed the occurrence of a magnetic phase transition in an atomically thin vdW magnet ($CrBr_3$) with a thickness down to 11 nm. The surface magnetization distributions at different temperatures were also determined quantitatively. Our method is nondestructive, is compatible with other measuring techniques, and can be used in the study of antiferromagnetic materials[25,34,35] as well as magnons and related surface magnetism in 2D magnets.

On can see the Supplementary Material for sample preparation, equipment setup, and a description of the magnetization density distribution reconstruction of the 2D material.

The data that support the findings of this study are available from the corresponding authors upon reasonable request.

Acknowledgments. This work was supported by the National Natural Science Foundation of China (Grant Nos. 81788101, T2125011, and 11874338), the National Key R&D Program of China (Grant No. 2018YFA0306600), Chinese Academy of Sciences (Grants Nos. XDC07000000, GJJSTD20200001, QYZDY-SSW-SLH004, and ZDZBGCH2021002), Anhui Initiative in Quantum Information Technologies (Grant No. AHY050000), and Fundamental Research Funds for the Central Universities.

References

[1] Zhong D, Seyler K L, Linpeng X, Cheng R, Sivadas N, Huang B, Schmidgall E, Taniguchi T, Watanabe K, McGuire M A, Yao W, Xiao D, Fu K M C and Xu X 2017 *Sci. Adv.* **3** e1603113
[2] Park J G 2016 *J. Phys.: Condens. Matter* **28** 301001
[3] Samarth N 2017 *Nature* **546** 216
[4] Song T, Cai X, Tu M W Y, Zhang X, Huang B, Wilson N P, Seyler K L, Zhu L, Taniguchi T, Watanabe K, McGuire M A, Cobden D H, Xiao D, Yao W and Xu X 2018 *Science* **360** 1214
[5] Cheng G and Xiang Z 2019 *Science* **363** eaav4450
[6] Gibertini M, Koperski M, Morpurgo A F and Novoselov K S 2019 *Nat. Nanotechnol.* **14** 408
[7] Huang B, Clark G, Navarro-Moratalla E, Klein D R, Cheng R, Seyler K L, Zhong D, Schmidgall E, McGuire M A, Cobden D H, Yao W, Xiao D, Jarillo-Herrero P and Xu X 2017 *Nature* **546** 270
[8] Gong C, Li L, Li Z, Ji H, Stern A, Xia Y, Cao T, Bao W, Wang C, Wang Y, Qiu Z Q, Cava R J, Louie S G, Xia J and Zhang X 2017 *Nature* **546** 265
[9] Burch K S, Mandrus D and Park J G 2018 *Nature* **563** 47
[10] Hao Y, Gu Y, Gu Y, Feng E, Cao H, Chi S, Wu H and Zhao J 2021 *Chin. Phys. Lett.* **38** 096101
[11] Deng Y, Yu Y, Song Y, Zhang J, Wang N Z, Sun Z, Yi Y, Wu Y Z, Wu S, Zhu J, Wang J, Chen X H and Zhang Y 2018 *Nature* **563** 94
[12] Huang B, Clark G, Klein D R, MacNeill D, Navarro-Moratalla E, Seyler K L, Wilson N, McGuire M A, Cobden D H, Xiao D, Yao W, Jarillo-Herrero P and Xu X 2018 *Nat. Nanotechnol.* **13** 544
[13] Jiang S, Li L, Wang Z, Mak K F and Shan J 2018 *Nat. Nanotechnol.* **13** 549
[14] Jiang P, Wang C, Chen D, Zhong Z, Yuan Z, Lu Z Y and Ji W 2019 *Phys. Rev. B* **99** 144401
[15] Song T, Fei Z, Yankowitz M, Lin Z, Jiang Q, Hwangbo K, Zhang Q, Sun B, Taniguchi T, Watanabe K, McGuire M A, Graf D, Cao T, Chu J H, Cobden D H, Dean C R, Xiao D and Xu X 2019 *Nat. Mater.* **18** 1298
[16] Sivadas N, Okamoto S, Xu X, Fennie C J and Xiao D 2018 *Nano Lett.* **18** 7658
[17] Zhang Z, Shang J, Jiang C, Rasmita A, Gao W and Yu T 2019 *Nano Lett.* **19** 3138
[18] Chen W, Sun Z, Wang Z, Gu L, Xu X, Wu S and Gao C 2019 *Science* **366** 983
[19] Zhang W B, Qu Q, Zhu P and Lam C H 2015 *J. Mater. Chem. C* **3** 12457
[20] Lovchinsky I, Sanchez-Yamagishi J D, Urbach E K, Choi S, Fang S, Andersen T I, Watanabe K, Taniguchi T, Bylinskii A, Kaxiras E, Kim P, Park H and Lukin M D 2017 *Science* **355** 503
[21] Fabre F, Finco A, Purbawati A, Hadj-Azzem A, Rougemaille N, Coraux J, Philip I and Jacques V 2021 *Phys. Rev. Mater.* **5** 034008
[22] Broadway D A, Scholten S C, Tan C, Dontschuk N, Lillie S E, Johnson B C, Zheng G, Wang Z, Oganov A R, Tian S, Li C, Lei H, Wang L, Hollenberg L C L and Tetienne J P 2020 *Adv. Mater.* **32** 2003314
[23] Nelz R, Radtke M, Slablab A, Xu Z Q, Kianinia M, Li C, Bradac C, Aharonovich I and Neu E 2020 *Adv. Quantum Technol.* **3** 1900088
[24] Shang Y X, Hong F, Dai J H, Lu Y N, Liu E K, Yu X H, Liu G Q and Pan X Y 2019 *Chin. Phys. Lett.* **36** 086201
[25] Gross I, Akhtar W, Garcia V, Martínez L J, Chouaieb S, Garcia K, Carrétéro C, Barthélémy A, Appel P, Maletinsky P, Kim J V, Chauleau J Y, Jaouen N, Viret M, Bibes M, Fusil S and Jacques V 2017 *Nature* **549** 252
[26] Wang C J, Li R, Ding B, Wang P, Wang W, Wang M, Guo M, Duan C K, Shi F and Du J 2020 *Appl. Phys. Lett.* **116** 184001
[27] Zhou B B, Jerger P C, Lee K H, Fukami M, Mujid F, Park J and Awschalom D D 2020 *Phys. Rev. X* **10** 011003
[28] Vool U, Hamo A, Varnavides G, Wang Y, Zhou T X, Kumar N, Dovzhenko Y, Qiu Z, Garcia C A C, Pierce A T, Gooth J, Anikeeva P, Felser C, Narang P and Yacoby A 2021 *Nat. Phys.* **17** 1216
[29] Solyom A, Flansberry Z, Tschudin M A, Leitao N, Pioro-Ladrière M, Sankey J C and Childress L I 2018 *Nano Lett.* **18** 6494
[30] Thiel L, Wang Z, Tschudin M A, Rohner D, Gutiérrez-Lezama I, Ubrig N, Gibertini M, Giannini E, Morpurgo A F and Maletinsky P 2019 *Science* **364** 973
[31] Sun Q C, Song T, Anderson E, Brunner A, Förster J, Shalomayeva T, Taniguchi T, Watanabe K, Gräfe J, Stöhr R, Xu X and Wrachtrup J 2021 *Nat. Commun.* **12** 1989
[32] Lado J L and Fernández-Rossier J 2017 *2D Materials* **4** 035002
[33] Tsubokawa I 1960 *J. Phys. Soc. Jpn.* **15** 1664
[34] Haykal A, Fischer J, Akhtar W, Chauleau J Y, Sando D *et al.* 2020 *Nat. Commun.* **11** 1
[35] Finco A, Haykal A, Tanos R, Fabre F, Chouaieb S *et al.* 2021 *Nat. Commun.* **12** 1

Supplemental Material

Magnetic phase transition in two-dimensional $CrBr_3$ probed by quantum sensor

Haodong Wang, [1,2,*] Peihan Lei, [1,2,*] Xiaoyu Mao, [1,3*] Xi Kong,[4,†] Xiangyu Ye, [1,2] Pengfei Wang, [1,2,5] Ya Wang, [1,2,5] Xi Qin, [1,2,5] Jan Meijer,[6] Hualing Zeng, [1,3,‡] Fazhan Shi, [1,2,5] Jiangfeng Du, [1,2,5,§]

[1] *Hefei National Laboratory for Physical Sciences at the Microscale and School of Physical Sciences, University of Science and Technology of China, Hefei 230026, China*

[2] *CAS Key Laboratory of Microscale Magnetic Resonance, University of Science and Technology of China, Hefei 230026, China*

[3] *CAS Center for Excellence in Quantum Information and Quantum Physics, University of Science and Technology of China, Hefei 230026, China*

[4] *National Laboratory of Solid State Microstructures and Department of Physics, Nanjing University, Nanjing 210093, China*

[5] *Felix-Bloch institute for solid state physics University Leipzig, Linnéstr. 5, D-04103 Leipzig, Germany*

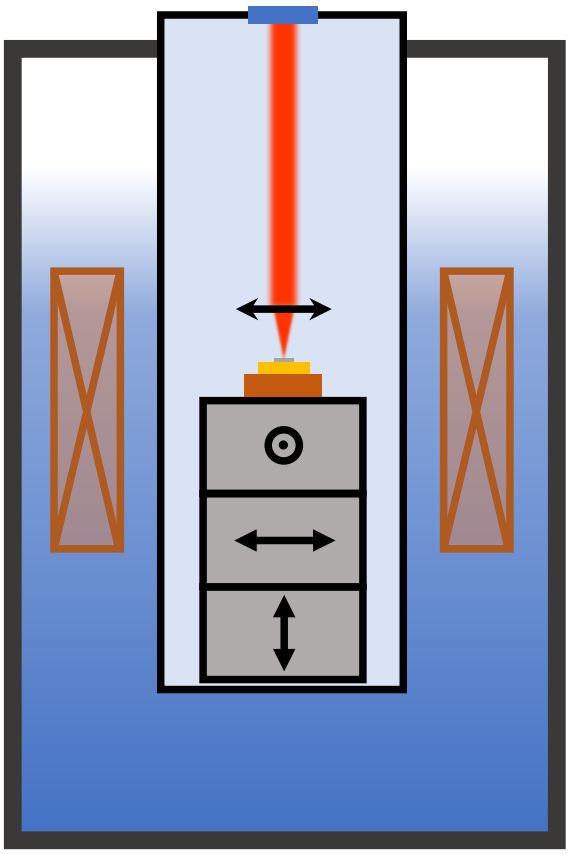

FIG. S1. The experimental apparatus. The vacuum cryostat is immersed in the liquid Helium with superconductor magnet. The diamond and the sample is put on a nanopositioner with a confocal system.

A. Sample preparations

Bulk single crystal CrBr3 and hBN in this study was purchased from HQ Graphene, Inc. The ultrathin CrBr3 and 200nm-thick-hBN were obtained by mechanical exfoliation on polydimethylsiloxane (PDMS) (Gel-Pak, WF-60-X4). Few-layer CrBr3 and monolayer hBN were prepared on PDMS by mechanical exfoliation method. Using the all-dry transfer method[1], hBN flake was transferred onto the surface of diamond right above the NV center layer. Monolayer CrBr3 was stacked on hBN in the same way. The sample e sample is transferred as quickly as possible into the vacuum light shield system to prevent sample decomposition.

B. Apparatus

The ODMR apparatus consist of a objective to focus 532 nm excitation laser on NV center, a microwave coplanar waveguide to deliver driving microwave electromagnetic field on NV centers and a 3-axis nano-stage to scan the sample. The whole sample-sensor system immerses in a liquid Helium-4 cryostat (Fig. S1). Three axis vector superconducting magnet are used to enable vectorial magnetic field control up to 1 T. The measurement temperatures were controlled from 4 K to 70 K by a feed-back thermometer placed close to the sample.

C. Magnetization density distribution reconstruction

We assume the magnetization has only perpendicular component under 200 mT. The method is performed in Fourier space with Fourier-space coordinates $k = (k_x, k_y)$ in the (x, y)-plane.

$$\nabla \times H = 0. \tag{1}$$

Considering the boundary condition of the half-space above the sample,

$$H(k, z) = -\nabla \left[\frac{\sigma(k, 0)}{2} e^{-kz} \right], \tag{2}$$

where $\nabla = (ik_x, ik_y, \partial/\partial z)$ is the gradient operator in Fourier space, $k = \sqrt{k_x^2 + k_y^2}$.

By using the method[2] on single spin probe situation, we can get magnetization distribution with ensemble of NV center. The resolution of our method, performed with ensemble NV sensor, is still limited by the Abbe diffraction limit $l = \lambda/\mathrm{NA}$=800 nm. Thus the high-frequency components of the map need to be filtered out.

REFERENCES

[1] A. Castellanos-Gomez, M. Buscema, R. Molenaar, V. Singh, L. Janssen, H. S. Van Der Zant, and G. A. Steele, "Deterministic transfer of two-dimensional materials by all-dry viscoelastic stamping," 2D Materials **1**, 011002 (2014).

[2] L. Thiel, Z. Wang, M. A. Tschudin, D. Rohner, I. Gutiérrez-Lezama, N. Ubrig, M. Gibertini, E. Giannini, A. F. Morpurgo, and P. Maletinsky, "Probing magnetism in 2D materials at the nanoscale with single-spin microscopy," Science **364**, 973–976 (2019).